

- <sup>6</sup>O. Sueoka and S. Koide, to be published.
- <sup>7</sup>I. K. MacKenzie and J. L. Campbell, Nucl. Instrum. Methods **101**, 149 (1972).
- <sup>8</sup>R. Paulin, R. Ripon, and W. Brandt, Phys. Rev. Lett. **31**, 1214 (1973).
- <sup>9</sup>A. Gainotti and C. Ghezzi, J. Phys. C **5**, 779 (1972).
- <sup>10</sup>B. Rozenfeld, A. Baranowski, and K. Jerie, Phys. Lett. **53A**, 154 (1975); F. Heinrich and A. Oggenfuss, Phys. Lett. **55A**, 441 (1976).
- <sup>11</sup>J. Bardeen and W. Shockley, Phys. Rev. **80**, 72 (1950).
- <sup>12</sup>G. Ottovani, C. Canali, and A. A. Quaranta, IEEE Trans. Nucl. Sci. **22**, 192 (1975).
- <sup>13</sup>K. Fujiwara, T. Hyodo, Y. Takakusa, and O. Sueoka, J. Phys. Soc. Jpn. **39**, 403 (1975).
- <sup>14</sup>The detectors were obtained from Princeton Gamma-Tech, Princeton, N. J. 08540.
- <sup>15</sup>We understand that these Ge crystals were supplied to Princeton Gamma-Tech by the General Electric Company, Philadelphia, Pennsylvania.
- <sup>16</sup>M. A. Shullman, G. M. Beardsley, and S. Berko, Appl. Phys. **5**, 367 (1975).
- <sup>17</sup>All the data shown in Fig. 2. were obtained with  $V_2 = 300$  V except for the  $V_1 - V_2 = 2800$ -V LN<sub>2</sub> datum for which  $V_2$  was 200 V. By observing the charge collection of the positron-induced pulses in the small detector it was determined that the electric field reaches the front surface of this detector ("punch through" occurs) when the bias is between 200 and 300 V. The electric field in the region where the positrons are stopping is therefore less than 100 V per 0.5 cm (the detector thickness) when the bias is 300 V.
- <sup>18</sup>Paul Norton and H. Levinstein, Phys. Rev. B **6**, 478 (1972).

### Concentration-Dependent Kohn Effect in Cubic Tungsten Bronzes\*

W. A. Kamitakahara, B. N. Harmon, J. G. Taylor, L. Kopp, and H. R. Shanks  
Ames Laboratory—ERDA and Department of Physics, Iowa State University, Ames, Iowa 50010

and

J. Rath

Department of Physics, University of Iowa, Iowa City, Iowa 52240

(Received 29 March 1976)

Inelastic neutron scattering measurements on single crystals of cubic Na<sub>x</sub>WO<sub>3</sub> reveal a large concentration-dependent Kohn anomaly in the [100] longitudinal acoustic-phonon dispersion curve. The results demonstrate the two-dimensional character of the Fermi surface, support the rigid-band model for  $0.56 < x < 0.83$ , and conflict with the percolation model which has just recently been proposed to explain the transport properties of the tungsten bronzes.

A pronounced, concentration-dependent Kohn effect has been observed in crystals of the non-stoichiometric compound Na<sub>x</sub>WO<sub>3</sub> for  $x$  values between 0.56 and 0.83. Comparisons of the shape and  $x$ -dependent position of the Kohn anomaly with first principles calculations of the NaWO<sub>3</sub> band structure and  $\vec{q}$ -dependent susceptibility  $\chi(\vec{q})$  yield two important conclusions: (1) The Fermi surface is characteristic of a two-dimensional metal in a restricted sense, and (2) the rigid-band model is valid for this system. The results suggest that for the investigation of certain wave-vector-dependent properties, Na<sub>x</sub>WO<sub>3</sub> can be useful as a prototype two-dimensional metal with the advantages (over real two-dimensional metals, the layered compounds<sup>1</sup>) of large, stable, single crystals and an easily variable electron concentration. In addition, the results are in direct conflict with the percolation model which has very recently been used to explain the

intriguing electronic-transport properties of Na<sub>x</sub>WO<sub>3</sub>.<sup>2</sup>

Sodium tungsten bronze, Na<sub>x</sub>WO<sub>3</sub>, has the cubic perovskite structure for  $x \geq 0.5$  above about 150°C. At lower temperatures in this concentration range there is a very small tetragonal distortion<sup>3</sup> which we neglect in the analysis of the experiments and the calculations described below. The neutron scattering measurements were performed on triple-axis spectrometers at the Ames Laboratory Research Reactor. The crystals, grown by fused-salt electrolysis<sup>4</sup> at the Ames Laboratory, were typically cubic in shape, with volumes of approximately 10 cm<sup>3</sup>. The [100] longitudinal acoustic-phonon dispersion curve was measured for three  $x$  values, determined from x-ray diffraction measurements of the lattice constant to be  $0.565 \pm 0.003$ ,  $0.593 \pm 0.002$ , and  $0.830 \pm 0.007$ . The majority of the data were taken at a fixed incident energy of 12.9 THz us-

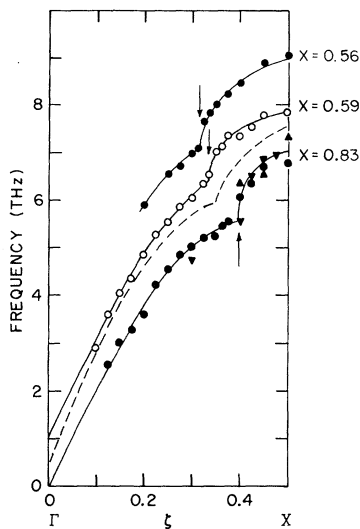


FIG. 1. The longitudinal acoustic-phonon dispersion curves for  $\text{Na}_x\text{WO}_3$  along the  $[100]$  direction. The curves for  $x = 0.56$  and  $0.59$  have been displaced upward by 2 THz and 1 THz, respectively (1 THz = 4.14 meV). The dashed curve is the simple model discussed in the text. The positions of the Kohn anomalies are indicated by arrows. The full width at half-maximum of a phonon peak was typically 1 THz.

ing the (002) planes of zinc and pyrolytic graphite as monochromator and analyzer. For  $x = 0.56$  and  $0.59$ , all points were measured at wave vector transfers  $\vec{q} = (2 + \zeta, 0, 0)2\pi/a$ , while for  $x = 0.83$ , measurements were made at  $\vec{q} = (3 + \zeta, 0, 0)2\pi/a$  and  $(3 - \zeta, 0, 0)2\pi/a$  to exclude the possibility that the effect arises from inelastic structure factors that transfer intensity from one branch to another. The data were further checked with the  $x = 0.59$  sample by performing measurements on a different spectrometer using a fixed scattered neutron energy of 6 THz. The phonon frequencies measured under different conditions were in good agreement. The results of these measurements are displayed in Fig. 1. A large anomaly occurs at  $\zeta = 0.315, 0.345, 0.395 \pm 0.010$  for  $x = 0.56, 0.59$ , and  $0.83$ , respectively.

Both the position and shape of the anomaly can be directly related to the electronic band structure. Qualitatively the electronic structure of the transition-metal perovskites is most easily described by a nearest-neighbor linear combination of atomic orbitals (LCAO) model.<sup>5,6</sup> The conduction band consists of tungsten  $t_{2g}d$  orbitals interacting with oxygen  $P_\pi$  orbitals. Because of the planar overlap between these orbitals, the corresponding bands are "two-dimensional" in the sense that they only depend on two compo-

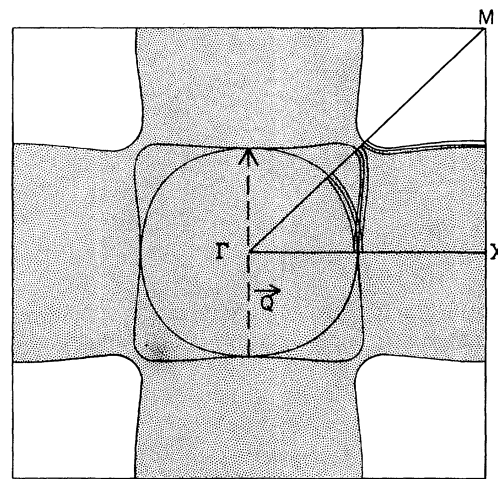


FIG. 2. Cross section of the Fermi surface in the (100) plane. The additional lines in the  $\Gamma XM$  section indicate the size of the rms error in the Fourier series fit to the calculated eigenvalues.

ments of the wave vector. This character of the conduction bands was first emphasized by Wolfgram, who used the simple LACO model to show that the two dimensionality accounted for the observed structure in the optical properties of  $\text{SrTiO}_3$ ,  $\text{BaTiO}_3$ , and  $\text{KTaO}_3$ . We have performed a first-principles Korringa-Kohn-Rostoker (KKR) calculation for cubic  $\text{NaWO}_3$ <sup>7</sup> in order to make quantitative comparisons with experiment. The bands are similar to those obtained by Mattheiss<sup>8,9</sup> for the isoelectronic compound  $\text{ReO}_3$  differing only in detail. The two-dimensional character is manifested in the Fermi surface which consists of three intersecting cylinders extending along the  $[100]$  directions. The three pieces shown in the cross section in the (100) plane (Fig. 2) are (i) the exterior parts of the two cylinders whose axes lie in the plane, (ii) a square formed by the intersection of these two cylinders, and (iii) a circle formed by the cross section of the cylinder perpendicular to the (100) plane. The cylinders are more nearly uniform in diameter than indicated in Fig. 2; part of the curvature comes from a Fourier fit to the calculated band structure. In the rigid-band model each sodium atom gives up one electron to the conduction band, and the volume or cylinder radius becomes smaller as  $x$  is decreased. The applicability of the rigid-band model is supported by the fact that an additional KKR calculation of cubic  $\text{WO}_3$  gives a band structure nearly identical to that obtained for  $\text{NaWO}_3$ ,<sup>7</sup> showing that the Na ion does not appreciably affect the electronic structure.

A Kohn anomaly may occur along a particular direction in the Brillouin zone when the wave vector of the phonons exceeds the Fermi-surface caliper in that direction. The effect is usually small, especially in low-electron-density metals which are not superconductors.<sup>10</sup> However, if large portions of the Fermi surface are spanned by the same wave vector  $\vec{Q}$ , as is quite evidently the case for  $\text{NaWO}_3$  (see Fig. 2), then the number of electrons contributing to the screening changes substantially as the phonon wave vector exceeds  $\vec{Q}$ . The effect of screening on the phonons can be illustrated by a simple model<sup>11,12</sup> (strictly valid only for one atom per unit cell) in which the longitudinal phonon frequency,  $\omega(\vec{q})$ , is changed to

$$\omega^2(\vec{q}) = \Omega^2(\vec{q}) - \frac{W^2(\vec{q})}{V(\vec{q}) + 1/\chi(\vec{q})}. \quad (1)$$

Here  $W(\vec{q})$  describes the electron-phonon interaction and  $V(\vec{q})$  the electron-electron interaction. Neither of these functions varies rapidly with  $\vec{q}$ , so that any very sharp feature in the phonon spectrum must come from the  $\vec{q}$  dependence of the susceptibility, which is given by

$$\chi(\vec{q}) = \sum_{\vec{k}} \frac{f(\vec{k}) - f(\vec{k} + \vec{q})}{E(\vec{k} + \vec{q}) - E(\vec{k})}, \quad (2)$$

where  $f(\vec{k})$  is the Fermi function. Although prominent anomalies may occur in the phonon spectrum which can be explained<sup>12</sup> by the  $\vec{q}$  dependence of  $W(\vec{q})$  and  $V(\vec{q})$ , the term Kohn anomaly refers only to a sharp feature in the dispersion relation which is generated by the singular behavior of  $\chi(\vec{q})$  at  $|\vec{q}| = 2k_F$ .

The  $\vec{q}$  dependence of the susceptibility is largely determined by the geometry of the Fermi surface.<sup>13</sup> For free-electron energy bands in three dimensions, the Fermi surface is a sphere and  $\chi(\vec{q})$  is the well-known Lindhard function. If the system is essentially one dimensional, the Fermi surface consists of parallel planes and  $\chi(\vec{q})$  is sharply peaked at  $q = 2k_F$ , generating a very strong Kohn effect<sup>14</sup> and an associated structural instability (Peierls instability). For free electrons in two dimensions, the Fermi surface is cylindrical and the susceptibility for  $\vec{q}$  perpendicular to the cylinder axis is easily evaluated, giving the curve labeled "analytic" in Fig. 3 for a cylinder of diameter  $\zeta = 0.35$ . The other curves in the figure are susceptibilities for  $\text{Na}_x\text{WO}_3$  derived from the KKR band structure via numerical methods<sup>15</sup> using only the three bands which cross

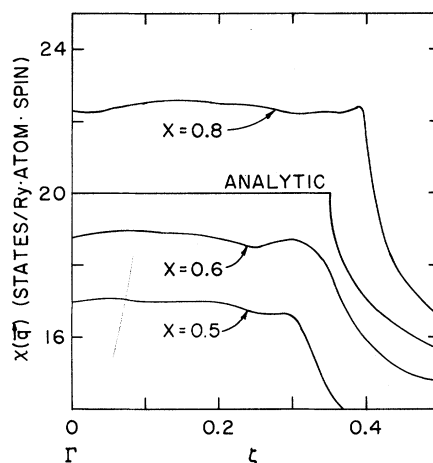


FIG. 3. The numerically calculated  $\vec{q}$ -dependent susceptibility of  $\text{Na}_x\text{WO}_3$  along the [100] direction for three different  $x$  values. The analytical curve is the result for a two-dimensional free electron system, with a constant ( $\vec{q}$ -independent) term added to account for the contribution from other bands.

the Fermi level. The resemblance between the analytic and numerically calculated curves is striking, particularly for  $x = 0.83$ .

Because the Fermi surface is not exactly cylindrical, the curves do have some rounding, due in part to a Fourier fit to the bands. A precise  $\vec{q}$  vector at which the Kohn anomaly is expected to occur may be obtained by a construction similar to that used to locate the experimental anomaly. The nearly horizontal section of the  $\chi(\vec{q})$  curve is extended to the right, while the curve from the zone boundary is extended upward to the left joining perpendicularly to the horizontal line at the predicted  $\vec{q}$  vector. It is found that this  $\vec{q}$  vector is exactly the  $X$ - $\Gamma$ - $X$  caliper (the vector  $\vec{Q}$  shown in Fig. 2). The theoretical  $X$ - $\Gamma$ - $X$  calipers for  $x = 0.56$ ,  $0.59$ , and  $0.83$ , using the rigid-band model, are  $aQ/2\pi = 0.332$ ,  $0.342$ , and  $0.404$ , respectively, in good agreement with experiment.

The shape of the observed anomalies can also be characterized by  $\chi(\vec{q})$  and is in fact the shape expected for a cylindrical Fermi surface.<sup>16</sup> The dashed line in Fig. 1 is an analytical curve obtained by adding the electronic contribution of Eq. (1) to a simple nearest-neighbor force-constant model [ $\Omega(\vec{q}) \sim \sin(qa/2)$ ]. The function  $W(\vec{q})$  was taken to be zero at  $q = 0$  and to increase roughly linearly with  $q$ , while  $V(\vec{q})$  was taken as a small constant divided by  $q^2$ . It should be emphasized that the shape of the Kohn anomaly will not depend on these functions as long as they are

slowly varying functions of  $\vec{q}$ . The function  $\chi(\vec{q})$  labeled "analytic" in Fig. 3 was used in Eq. (1). The sharpness and general shape of the anomaly is governed strictly by  $\chi(\vec{q})$ , whereas the size of the anomaly is enhanced by a favorably large electron-phonon interaction and a small effective electron-electron interaction. Thus the observed shape of the anomaly provides further evidence for the correctness of our  $\chi(\vec{q})$  calculations and for the two-dimensional character which they imply.

Finally we wish to point out the significance of our results in connection with a recently proposed model for the alkali-tungsten bronzes.<sup>2</sup> In an impressive application of percolation theory, Webman, Jortner, and Cohen were able to explain the normal-state transport properties of  $\text{Na}_x\text{WO}_3$  by assuming a nonrandom clustering of the Na ions into local metallic regions about 45 Å in diameter in which  $x_{\text{local}} = 1$ . This model neglects structural changes in the lattice, and explains the semiconductor-to-metal transition near  $x = 0.2$  as the onset of continuous percolation in which a finite fraction of the metallic regions are continuously connected across a macroscopic sample. Since electrons would be trapped by the Madelung potential of the local  $x = 1$  sodium regions, the electron concentration in these regions would also correspond to  $x = 1$ . This is in direct conflict with our results which corroborate the rigid-band model for  $x \geq 0.56$ , and indicate the electrons are delocalized throughout the crystal. In addition, recent x-ray diffraction measurements by Takusagawa and Jacobson<sup>17</sup> show that in tetragonal  $\text{Na}_{0.33}\text{WO}_3$ , the sodium atoms are completely ordered and no local  $x = 1$  regions can exist. We thus conclude that the percolation model is not applicable to the  $\text{Na}_x\text{WO}_3$  system and that the  $x$  dependence of the transport properties must have another explanation. In particular we believe that the electron-phonon interaction is strongly influenced by structural considerations, as recently emphasized by Ngai and Silbergliitt<sup>18</sup> in their discussion of supercon-

ductivity in the  $T1$  tetragonal structure of  $\text{Na}_x\text{WO}_3$  ( $0.2 < x < \sim 0.4$ ).

\*Work performed for the U. S. Energy Research and Development Administration under Contract No. W-7405-eng-82.

<sup>1</sup>Kohn anomalies have been observed in neutron scattering experiments on layered compounds by N. Wakabayashi, H. G. Smith, and H. R. Shanks, *Phys. Lett.* **50A**, 367 (1974); and by D. E. Monton, J. D. Axe, and F. J. diSalvo, *Phys. Rev. Lett.* **34**, 734 (1975).

<sup>2</sup>I. Webman, J. Jortner, and M. H. Cohen, *Phys. Rev. B* **13**, 713 (1976).

<sup>3</sup>G. Bonera, F. Borsa, M. L. Crippa, and A. Rigamonti, *Phys. Rev. B* **4**, 52 (1971); F. Borsa, in *Local Properties at Phase Transitions*, edited by K. A. Müller and A. Rigamonti (North-Holland, Amsterdam, 1976). The structural distortion suggested in the latter paper has recently been observed by neutron diffraction (W. A. Kamitakahara, unpublished).

<sup>4</sup>H. R. Shanks, *J. Cryst. Growth* **13/14**, 433 (1972).

<sup>5</sup>J. M. Honig, J. O. Dimmock, and W. H. Kleiner, *J. Chem. Phys.* **50**, 5232 (1969).

<sup>6</sup>T. Wolfram, *Phys. Rev. Lett.* **29**, 1383 (1972).

<sup>7</sup>L. Kopp, S. H. Liu, and B. N. Harmon, to be published.

<sup>8</sup>L. F. Mattheiss, *Phys. Rev.* **181**, 987 (1969).

<sup>9</sup>L. F. Mattheiss, *Phys. Rev. B* **2**, 3918 (1970).

<sup>10</sup>G. Nilsson and S. Rolandson, *Phys. Rev. B* **9**, 3278 (1974).

<sup>11</sup>D. Pines, *Elementary Excitation in Solids* (Benjamin, New York, 1964).

<sup>12</sup>S. K. Sinha and B. N. Harmon, *Phys. Rev. Lett.* **35**, 1515 (1975).

<sup>13</sup>W. E. Evenson and S. H. Liu, *Phys. Rev.* **178**, 783 (1969).

<sup>14</sup>See, for example, J. W. Lynn, M. Iizumi, G. Shirane, S. A. Werner, and R. B. Sallaint, *Phys. Rev. B* **12**, 1154 (1975), and references contained therein.

<sup>15</sup>P.-A. Lindgård, *Solid State Commun.* **16**, 481 (1975); J. Rath and A. J. Freeman, *Phys. Rev. B* **11**, 2109 (1975).

<sup>16</sup>A. M. Afanas'ev and Yu. Kagan, *Zh. Eksp. Teor. Fiz.* **43**, 1456 (1962) [*Sov. Phys. JETP* **16**, 1030 (1963)].

<sup>17</sup>F. Takusagawa and R. A. Jacobson, to be published.

<sup>18</sup>K. L. Ngai and R. Silbergliitt, *Phys. Rev. B* **13**, 1032 (1976).